Synthetic Metals 307 (2024) 117694

Contents lists available at ScienceDirect

Synthetic Metals

journal homepage: www.elsevier.com/locate/synmet

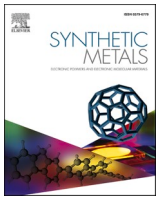

Exploring novel methods: Acid treatment, metal nanoparticle doping, and graphene insertion for enhanced electrical conductivity of nm thin PEDOT:PSS films

Amrita Chakraborty, Aaron DiFilippo, Sheena Deivasigamani, Calvin Hong, Anshu Madwesh, Marius Orlowski *

Bradley Department of Electrical and Computer Engineering, Virginia Tech, Blacksburg, VA 24061, USA

ARTICLE INFO

Keywords:
Conducting polymers
PEDOT:PSS
Metal nanoparticles
Topical and bulk doping
Monolayer and trilayer graphene

ABSTRACT

This study builds upon our previous research aimed at enhancing the electrical conductivity of Poly(3,4-ethylenedioxythiophene) Polystyrene Sulfonate (PEDOT:PSS). We investigate a range of techniques, including acid treatments, doping with metal nanoparticles (Cu and Ag), deposition of multiple PEDOT:PSS layers, and incorporation of mono/multiatomic layer graphene. Our investigations reveal that optimizing the deposition of PEDOT:PSS multilayers and treating them with nitric acid yields superior results compared to alternative methods employing metal nanoparticles and graphene. This optimized process not only enhances the electrical conductivity of PEDOT:PSS but also offers advantages in terms of reduced errors, increased stability, and cost-effectiveness when compared to the use of graphene layers and metal nanoparticles. Optimization parameters such as spinning speed, etchant concentration, and etching time are crucial factors in achieving these outcomes. Compared to single-layer PEDOT:PSS films of the same thickness, the optimized nine-layer PEDOT:PSS treated with nitric acid demonstrates a significant enhancement of conductivity from 0.18 S/cm to 15,699 S/cm. Furthermore, we address film aging to mitigate reliability issues induced by ambient conditions.

1. Introduction

In our previous study [1], we introduced a novel method for producing conductive organic electrodes using doped PEDOT-PSS polymer films. Here, we focus on the PEDOT:PSS

polymer, although there are many alternative polymers such as P3HT [1] or polypyrrole (Ppy) [2]. The preferred use of an alternative polymer depends on specific applications. For instance, the stability of the conducting polymer layer on the electrode is critical for many applications, including biosensors. Reference [2] reports a successful electrochemical synthesis of a Ppy film on a gold surface, enabling biomedical applications in scaffold design and environmental tasks such as the development of semi-permeable membranes for water purification.

In the past, numerous methods to enhance the conductivity of PEDOT:PSS have been proposed, with many investigations conducted by the Ouyang group [3–8]. It was reported that treating PEDOT:PSS with ethylene glycol solvent increased the conductivity from 0.2 S/cm to 200 S/cm [3]. Treatment with a cosolvent of water and organic solvents such as ethanol, isopropyl alcohol, acetonitrile, acetone, and tetrahydrofuran increased the conductivity of PEDOT:PSS to a maximum of 103 S/cm [4]. Additionally, treatment with the amphiphilic fluoro compound hexafluoroacetone increased the conductivity to 1325 S/cm [5]. A 2015 review article [6] reported that treatment with H_2SO_4 increased the conductivity to 3000 S/cm. Enhanced thermoelectric properties of PEDOT:PSS with common acids and bases for direct energy harvesting have also been documented [7], with optimal PEDOT:PSS films displaying a Seebeck coefficient of 39.2 μV/K and a conductivity of 2170 S/cm at room temperature, resulting in a power factor of 334 $\mu W/(m \cdot K^2)$.

A recent review article comprehensively summarized the basic principles of functionalized PEDOT films for optoelectronics and thermoelectronics, reporting conductivities exceeding 4100 S/cm for acid-treated PEDOT:PSS [8]. PEDOT:PSS films treated with 100 % H_2SO_4, followed by annealing at an optimized drying temperature of 120°C, achieved a conductivity of 4380 S/cm [9]. However, this method suffers

* Corresponding author.
E-mail address: m.orlowski@vt.edu (M. Orlowski).

https://doi.org/10.1016/j.synthmet.2024.117694
Received 17 May 2024; Received in revised form 7 July 2024; Accepted 8 July 2024
Available online 20 July 2024

from a very narrow processing window. Yeon et al. [10] identified a very stable and manufacturable process for enhancing the conductivity of PEDOT:PSS by treating the polymer with HNO_3 at room temperature, yielding a conductivity as high as 4100 S/cm.

Our previous findings [1] revealed the extraordinary potential of PEDOT:PSS electrodes, showcasing their ability to be patterned and robust adhesion to diverse substrates, ranging from oxidized silicon wafers to flexible materials like Mylar. Effective substrate adhesion was achieved through a simple oxygen plasma cleaning step. To pattern the PEDOT:PSS films, we introduced a sacrificial silver metal layer to prevent chemical deterioration of PEDOT:PSS when exposed to standard photolithography process solvents. Key findings from reference [1] include a remarkable increase in electrical conductivity (by over two orders of magnitude) through multiple PEDOT:PSS depositions, without a significant increase in film thickness. An exponential relationship emerged as we observed a fundamental dependency between sheet resistance and the number of PEDOT:PSS coatings, deepening our understanding of the roles of PEDOT (the conductive component) and PSS (the non-conductive component) within the deposited PEDOT:PSS material. In the absence of other enhancement techniques, additional PEDOT:PSS coatings beyond six layers yield diminishing returns in terms of lowering the sheet resistance. However, in conjunction with acid treatments investigated in this study, the point at which only negligible improvements are obtained increases to about 9–10 coatings to compensate for the material loss due to acid treatment.

Furthermore, in our previous work [1], we explored the introduction of Cu nanoparticles (Cu NPs) as a doping agent, applied topically to soft-baked PEDOT:PSS films, revealing another remarkable leap in electrical conductivity—again, by two orders of magnitude. However, we encountered a notable counteractive effect: the two methods of conductivity enhancement, multiple PEDOT:PSS coatings, and Cu NP doping, did not simply add up as anticipated. In other words, combining these two methods did not yield cumulative improvements.

In earlier studies, the addition of metal nanoparticles to PEDOT:PSS has attracted a lot of interest. For example, X. Zhang et al. [11] successfully produced PEDOT:PSS thin films doped with silver nanoparticles (Ag NP) using inkjet printing, resulting in remarkable electrical and optical capabilities. In a similar vein, Patil et al. [12] reported that doping PEDOT:PSS with Ag NP increased its conductivity. R.-C. Zhang et al. [13] demonstrated the effectiveness of gold nanoparticle-PEDOT:PSS nanocomposites as catalysts in alkaline direct ethanol fuel cells by introducing a simplified synthesis procedure for their creation. Moreover, O. Ghazy et al. [14] used silver particles produced by gamma radiation to improve PEDOT:PSS conductivity, especially when it came to organic solar cells. Finally, strong evidence of notable improvements in polymer conductivity when Cu NPs were used as dopants was presented by L. Pham et al. [15].

In this paper, we continue our exploration of ways to enhance electrical conductivity of PEDOT:PSS layers and present novel techniques that extend and complement our previous work. Specifically, we examine treatments with nitric, phosphoric, and sulfuric acids, along with the effects of introducing noble metal nanoparticles and mono- and multi-layer graphene. In case of the acid treatment methods, nitric acid treatment emerges as a standout performer among the acid treatments, with its optimization as a focal point in our investigation. We have also examined how environmental conditions affect the organic electrodes treated by acids by storing them in standard laboratory conditions and vacuum chambers for up to two weeks.

The use of acids to enhance the conductivity of PEDOT:PSS films has been explored in previous studies. Phosphoric acid treatment of individual PEDOT:PSS films was applied for 0.5 and 10 minutes in a study by Wang et al. [16]. Their research showed that the PSS component could be efficiently eliminated by using phosphoric acid, which improved electron extraction and improved solar cell device performance [16]. They came to the conclusion that too much PSS impaired the gadgets' ability to gather electrons. Our findings corroborate this judgment and imply that treating solar cells with nitric acid may improve their efficiency even further. F. Zhang's group also demonstrated the production of semitransparent polymer solar cells (PCS) with a power conversion efficiency of 9.40 % and a visual transmittance of 24.6 % in their research [17]. Additionally, they tuned PCS to have a 15.6 % power conversion rate, showing poor transmittance in the near-infrared spectrum and high transmittance in the visible light range [18]. Additionally, Z. Xie et al. [19] showed how to use a post-spin-rinsing technique to produce highly conductive PEDOT:PSS transparent electrodes for polymer solar cells. In our earlier research, we investigated the application of Cu NPs topically and discovered that bulk doping of Cu was ineffective due to oxidation in aqueous solutions. In this new study, we employ noble metal nanoparticles, specifically silver (Ag), which facilitate beneficial bulk doping of the PEDOT:PSS layers.

In this paper, we also explore the insertion of graphene monolayers and trilayers to enhance the conductivity of PEDOT:PSS. Graphene has been previously employed in various forms to enhance the electrical conductivity of PEDOT:PSS films, resulting in significant improvements. In reference [20], PEDOT:PSS films were doped with graphene composites for applications in energy harvesting systems. The graphene composites were dispersed in a solution of PSS, and their content was varied to obtain the highest electrical conductivity. A 41 % improvement in conductivity was achieved over undoped PEDOT:PSS. Overall, the conductivity improvement led to a 93 % higher power factor than the device based on pristine PEDOT:PSS. A similar doping technique of PEDOT:PSS with graphene composites, combined with treatment of concentrated H_2SO_4, has been employed by M. Zhang [21] to enhance the electrocatalytic activity for the oxygen reduction reaction at the cathodes of fuel cells and metal-air batteries. The resultant PEDOT:PSS/graphene composites exhibit synergistically enhanced electrocatalytic activity, better tolerance to the methanol crossover effect and CO poisoning, and improved durability over that of a Pt/C electrode.

Doping of PEDOT:PSS with reduced graphene oxide-carbon nanotubes has been used by P.C. Mahakul et al. [22] to enhance the conductivity of the polymer films for transparent electrode applications. A maximum conductivity of 3804 S/cm has been observed, which is comparable to that of indium tin oxide (7800 S/cm). In reference [23], PEDOT:PSS films were doped with graphene and graphene quantum dots, showing that both graphene and graphene quantum dots improve the conductivity of PEDOT:PSS films with only a small decrease in transparency (13–14 %).

Stable and highly conductive polymer films have been obtained by D. Liu et al. [24] by doping PEDOT:PSS with graphene nanocomposites for biosensor applications. Graphene nanoplatelet (GNP) composites were deposited on fluoride tin oxide (FTO) via the electrospray technique from a mixture solution of PEDOT:PSS and GNPs, which was subsequently treated with H_2SO_4 acid. Such an enhanced FTO electrode showed very high catalytic activity for the detection of dopamine, easily differentiating the electrochemical oxidation signals of ascorbic and uric acids.

S.H. Ko et al. [25] demonstrated a flexible sensor with graphene oxide/PEDOT:PSS composites for voltammetric determination of selective low levels of dopamine. The sensor showed a dopamine detection limit of 0.008 μM and a sensitivity of 69.3 $\mu A/\mu Mcm^2$.

F-P. Du et al. [26] achieved high conductivity polymer films by doping PEDOT:PSS with graphene quantum dots (GQD). An electric conductivity of 71.72 S/cm was observed, which is 31 % higher than that of pristine PEDOT:PSS. The thermal conductivity experienced an even higher improvement of 113 % than that of pristine PEDOT:PSS. PEDOT:PSS/GQDs were prepared via a simple casting method. The strong π-π bonding between GQDs and PSS chains led to decoupling and phase separation of PEDOT:PSS and PSS chains, resulting in higher electrical and thermal conductivities.

M.A. Badri et al. [27] combined PEDOT:PSS with exfoliated graphene to provide an alternative to indium tin oxide in optoelectronic devices. The graphene flakes were synthesized via the graphite

exfoliation method. A good compromise, as a function of the graphene content, was achieved, with the conductivity and optical transparency as high as 4.2×10^3 S/cm and 94 %, respectively.

In reference [19,28], an electrochromic device was successfully fabricated using PEDOT:PSS and graphene as active, flexible conductive electrode films. In their work, S.K Nemani [28] harnessed the wrinkling instability of graphene to impart hydrophobic properties to the electrode. A wide range of color contrast, flexibility, and anti-wetting nature of the device has been achieved. A comprehensive review of various doping techniques of PEDOT:PSS with graphene and its derivatives, such as graphene oxide, reduced graphene oxide, and graphene quantum dots, has been given by G. J. Adekoya et al. [29]. Recent advances in the integration of PEDOT:PSS with graphene and its derivatives for applications in energy storage devices, such as supercapacitors, have been described in much detail by O. Faruk et al. [30].

Our objective of the continuation of the precursor work [1] work is also to assess the compatibility of various conductivity enhancement methods and explore potential synergies among them. The dispersion of silver nanoparticles, whether applied topically or introduced as bulk doping, reveals promising effects—though interestingly, their conjunction with acid treatment does not yield further major enhancements.

The main objective of this paper is to develop organic electrodes embedded with copper or silver particles for nonvolatile ReRAM memory arrays on flexible substrates. It is well-established that ReRAM arrays function optimally when constructed with Cu and Ag particles as building components for the filaments connecting the two electrodes of a ReRAM cell. Given our focus on organic ReRAM memory, other properties of these films, such as transparency, are not pertinent to our application. Consequently, no analysis of the transmittance of the multilayer PEDOT:PSS has been conducted. However, favorable transparency characteristics could prove advantageous if, in the future, our organic memory arrays were to be integrated with solar cells for power supply purposes.

The present paper's structure is as follows: In the *Electrode Fabrication* section, we begin by briefly summarizing the fundamental manufacturing steps involved in depositing and patterning PEDOT:PSS layers, along with the methods to enhance the electrical conductivity of these films, which were previously covered in our earlier paper [1]. We then shift our focus to providing a detailed account of the acid treatment process using and the preparation, application of Ag and Cu NP dispersions, and insertion of mono- and multilayer graphene.

Moving on to the *Results* section, we first present the individual effects of nitric, phosphoric, and sulfuric acids (HNO_3, $H3PO_4$, and H_2SO_4) as well as the effects of topical and bulk doping of PEDOT:PSS with silver nanoparticles. In this initial part, we concentrate on the outcomes of each technique in isolation. Subsequently, in the latter part of the *Results* section, we delve into the synergistic effects that emerge when these techniques are combined with the multi-layer PEDOT:PSS deposition process. Finally, we summarize the most significant findings of the paper in the *Concluding Remarks* section.

2. Electrode fabrication

The fabrication of organic electrodes commenced with the utilization of a commercial dispersion of PEDOT:PSS in water. This dispersion was employed to deposit organic films onto cleaned substrates, which included oxidized Si wafers and flexible Mylar substrates. We utilized the spin-coating technique for film deposition, with the spin speed ranging from 500 rpm to 3000 rpm. This choice of spin speed was especially crucial for multilayer PEDOT:PSS stacks, where each layer's speed, including speed ramps, had to be carefully selected to achieve the desired film thickness and the highest conductivity. The subsequent application of oxygen plasma cleaning significantly enhanced the uniformity of these films.

To measure the film thickness accurately, the PEDOT:PSS films have been patterned to form a step. In the previous paper [1], we showcased the patterning of highly conductive polymer films using photolithography. This process employed a novel flow that relied on sacrificial metal layers. We successfully addressed adhesion issues and demonstrated that, with carefully calibrated process recipes, highly conductive PEDOT:PSS films can be patterned on both Si-wafer and flexible substrates like Mylar. This advancement opens avenues for the deployment of flexible electronics. Dektak profilometer and Atomic Force Microscopy (AFM) were utilized to determine the thickness of PEDOT:PSS films, yielding thickness differentials results of +/-1 nm. An optical microscopy image of a step of a patterned PEDT:PSS film is given in Fig. 1(a) along with the AFM image of the measurement of the film's thickness by AFM shown in Fig. 1(b). The thickness of the PEDOT:PSS layer depends on the spinning speed and on the numbers of PEDOT:PSS coatings, as shown in Table 1. A 3×PEDOT:PSS, for example, deposited at speeds of 1500, 2000, and 3000 rpm, for the 1st, 2nd, and 3rd deposition results in a total film thickness of 72 nm, which is at variance with the purely additive sum of 65+56+29=150 nm and merely 7 nm thicker than a 1×PEDOT:PSS (65 nm) spun at 1500 rpm.

To pattern the PEDOT:PSS, we employed protective layers, specifically PVD-deposited silver (Ag) thin films. These layers were instrumental during photolithography, safeguarding the film from UV light exposure and chemical reagents. The photolithography process encompassed exposing the desired pattern and subsequently developing the image reversal photo resist AZ 5214E-IR. Following this, the exposed Ag regions underwent etching using an HNO_3:H_2O solution. This step was followed by rinsing and the subsequent removal of the PEDOT:PSS layer through oxygen plasma treatment. In essence, the previous work [1] encompassed critical stages in the PEDOT:PSS film fabrication process, spanning deposition and uniformity measurement to precise photolithography-based patterning, with a specific emphasis on achieving superior electrical conductivity.

In the pursuit of optimizing acid treatment techniques for PEDOT:PSS samples, we conducted a comparative study involving three acids: phosphoric, sulfuric, and nitric, with concentrations ranging from 0 % to 100 %. The duration of the acid treatment was varied from 1 second to 60 seconds. Our protocol involved employing each acid at a 100 % concentration level, coupled with a brief 2-second treatment duration, which induced a significant enhancement of conductivity of PEDOT:PSS. In this initial experiment, the acid treatment was applied exclusively to a single layer of the PEDOT:PSS material. The acid method starts with the precise measurement of the desired acid concentration, followed by immersing PEDOT:PSS Si-wafer samples into the acid solution for the specified duration. Subsequently, the samples are promptly rinsed in DI water to eliminate any residual acid traces, ensuring the integrity of the results.

Regardless of whether the acid treatment targets a single or multiple layers of PEDOT:PSS, its core action involves the removal of PSS from the upper layer. The residue comprises a layer primarily composed of PEDOT, occasionally housing residual PSS inclusions, as illustrated in Fig. 2. Thus, after etching, the PSS component is largely removed, leaving predominantly the PEDOT component. It should be noted that methods for directly depositing PEDOT electrochemically have been

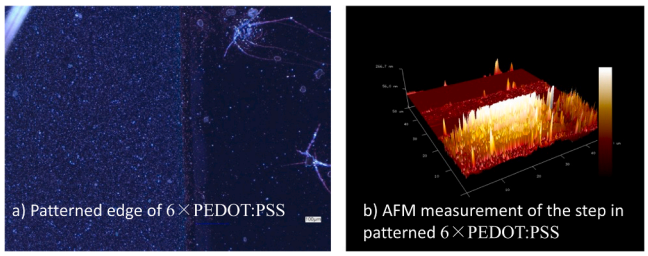

Fig. 1. a) Optical microscopy image of the patterned edge of a 6×PEDOT:PSS stack. b) AFM image of the step in the 6×PEDOT:PSS stack to measure the film thickness.

Table 1
The effective film thickness [nm] at different spinning speeds for 1×PEDOT:PSS, 3×PEDOT:PSS, 6×PEDOT:PSS, and 6×PEDOT:PSS stacks.

PEDOT:PSS # Speed in rpm	1× 1500	1× 2000	1× 3000	3× 1500,3000,1500	3× 1500,2000,3000	6× 1500,2000,4×3000	9× 1500, 2000,7×3000
Thickness [nm]	65	56	29	85	72	109	128

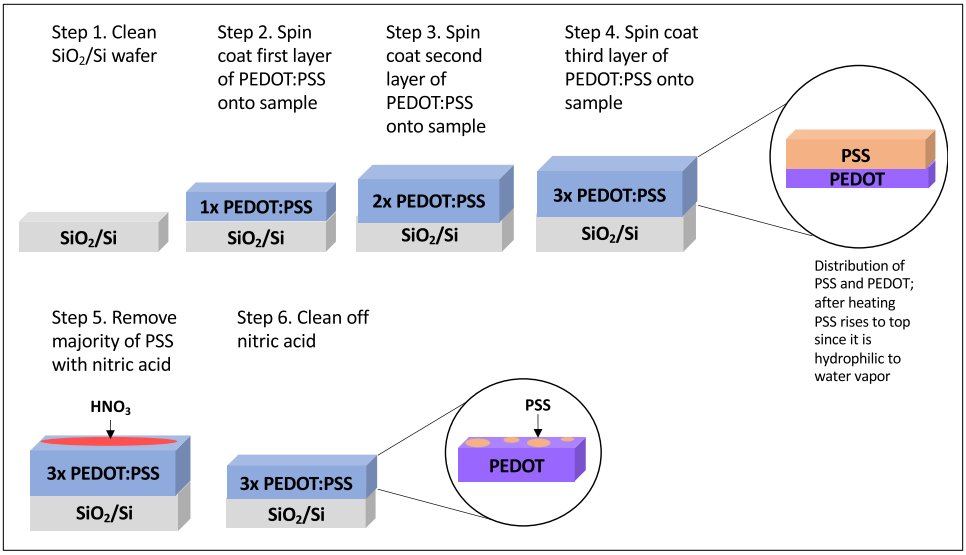

Fig. 2. Process steps of acid treatment of multilayer PEDOT:PSS films. The acid treatment results in removal of the top portion of PSS leaving only PSS inclusions within the PEDOT phase.

reported in the past [31]. Additionally, it has been demonstrated that the conjugation of polyaniline (PANI) with PEDOT enhances conductivity. This PANI-PEDOT copolymer has been effectively utilized in the design of pH sensors and gas sensors for CO_2 and NH_3 [31]. More recently, the group led by Ramanavičienė [32] reported a significant enhancement of the electrochromic properties of the PANI-PEDOT layer, achieved by incorporating gold nanostructures deposited on indium tin oxide-coated glass (ITO).

We conducted experiments involving the application of silver nanoparticles (Ag NPs) to multilayer PEDOT:PSS using both the topical and bulk doping approaches. For bulk doping, 5 mg of Ag NPs was combined with 10 ml of PEDOT:PSS solution to make a 0.5 mg/ml concentration solution. The mixture was stirred for a minimum of 1 hour and subsequently sonicated for an additional hour. In contrast, for surface doping, a dispersion solution of Ag NPs in ethanol of same 0.5 mg/ml concentration was prepared, followed by the same stirring and sonication procedure employed in the bulk doping method. The dispersion of Ag nanoparticles in ethanol was subsequently spin-coated onto the surface of the PEDOT:PSS layer at 1500 rpm. It should be mentioned in this context that it was established [4] that ethanol by itself leads to a modest increase of conductivity of the PEDOT:PSS.

The choice of silver nanoparticle concentration at 0.5 mg/ml was informed by our earlier research involving copper nanoparticles [1]. In a prior study, we explored different concentrations of Cu NPs, specifically 0.2 mg/ml and 0.5 mg/ml, and determined that the latter (0.5 mg/ml) yielded the most favorable outcomes. To maintain consistency, we opted for the same concentration (0.5 mg/ml) when working with silver nanoparticles

Regarding the silver nanoparticles, we had access to two powders from Sky Springs Nanomaterials, Inc., one with nanoparticles sizes ranging from 20 to 30 nm and another one with nanoparticles ranging from 50 to 60 nm, with the larger sizes providing higher conductivity of the PEDOT:PSS (see next section).

In this paper, the ultimate enhancement method under consideration entails the insertion of mono- and trilayer [33] graphene between the oxidized Si wafer and PEDOT:PSS films. Our transfer process for the graphene monolayer consisted of several steps:

1. Cutting polyethylene terephthalate (PET) and the graphene-on-copper sheet into 1 cm x 1 cm squares and taping the graphene-on-copper sheet onto the PET.
2. Spin-coating the polymethyl methacrylate PMMA solution onto the graphene at 500 RPM for 5 seconds, followed by 2500 RPM for 45 seconds. The PMMA solution comprised 10 ml of PMMA solution mixed with 10 ml of anisole solvent, resulting in a final concentration of 4.5 % PMMA. Approximately 4–5 drops of this PMMA solution were dispensed onto the graphene and spin-coated. An annealing step followed, with options including 50°C for 2 minutes.
3. Subsequently, PET was removed, and the sample was exposed to oxygen plasma at 30 W of power, with a gas flow rate of 10 SCCM of oxygen gas, for 1 minute.
4. The copper foil was then etched away by floating it in a copper etchant ($FeCl_3$) for approximately 10 minutes until most of the copper was etched away.
5. The film was transferred into DI water using a glass slide, left in the DI water for about 10 minutes, and this process was repeated two more times with fresh DI water each time.
6. After the third DI bath, the graphene film was lifted onto the oxidized Si wafer sample, effecting the transfer of graphene onto the wafer.
7. The sample was then air-dried for 4 hours and placed in a vacuum chamber for 12–24 hours.
8. The PMMA was then removed, by initially baking the wafer at 85°C for 5 minutes, followed by a bake at 140°C for 15 minutes and then subsequently immersing the sample in warm acetone at 55°C for 1 hour.
9. Finally, the sample was cleaned with isopropyl alcohol cleaning solvent (IPA) for 30 minutes and dried to obtain graphene on oxidized Si wafer.

This comprehensive process ensured the successful transfer of the

graphene monolayer onto the wafer. Fig. 3 shows the image a monolayer graphene transferred onto an oxidized Si substrate. The graphene trilayer is provided as a separate sample on 1 cm × 1 cm pieces of oxidized Si wafers by the company, Graphenea [33]. It consists of three graphene monolayers stacked directly upon each other.

The sheet resistance, denoted as R_{sq}, or the conductivity, symbolized as σ, of the PEDOT:PSS layers has been determined utilizing the four-probe measurement method [34]. The electrical properties, conductivity, and sheet resistance are related and can be expressed through Eq. (1):

$$\sigma = \frac{1}{R_{sq} \times t} \quad (1)$$

For instance, let's take a pristine PEDOT:PSS film deposited at 2000 rpm, resulting in a film thickness (t) of 56 nm and possessing a sheet resistance of R_{sq} equal to 1 MΩ/sq. According to Eq. (1), this sheet resistance value corresponds to a conductivity (σ) value of 0.18 S/cm.

3. Experimental results and discussion

We begin our investigation by examining the impact of acid treatment on a single-layer PEDOT:PSS, specifically utilizing phosphoric, sulfuric, and nitric acid. Literature reports indicate that the conductivity of PEDOT:PSS films treated with 100 % H_2SO_4, followed by annealing at an optimized drying temperature of 120°C, can reach a high conductivity of 4380 S/cm [9], which is nearly comparable to those of ITO and Al- or Ga-doped ZnO [35,36]. Additionally, [9] noted that a significant structural transition occurs in the PEDOT:PSS films when H_2SO_4 treatment exceeds an 80 % concentration. However, it was later pointed out that the narrow temperature range around the optimum of 120°C is too restrictive to achieve reproducible results [10]. Instead, [10] discovered that treating PEDOT:PSS with HNO_3 at room temperature yields a conductivity as high as 4100 S/cm. This study also reported that 14 M HNO_3 reduced the PEDOT:PSS film thickness by 66 %, while a weaker concentration of 3 M HNO_3 reduced the film thickness by approximately 50 %. In our work, Table 2 compares the film thicknesses of multi-coated PEDOT without acid treatment and with 60 % HNO_3 treatment. The data shows that the acid treatment significantly reduces the film thickness, corroborating the findings in [10].

As highlighted in [10], the conductivity enhancement depends on the concentration of HNO_3 rather than the treatment time. Material and morphology studies [10] confirmed the removal of PSS and the formation of highly ordered and densely packed PEDOT:PSS films. Consequently, the PEDOT-rich chains align in a preferred orientation, facilitating stronger inter-chain interactions between the conducting polymers. This alignment results in a lower energy barrier for inter-chain and inter-domain charge hopping, thereby enabling easier charge transfer among the PEDOT chains [10].

Table 2 and Table 3 presents the conductivity values obtained for these three acid treatments at a concentration of 100 % for 2 seconds.

Fig. 3. Graphene monolayer transferred onto SiO_2/Si following the procedure outlined in the text.

Table 2
thickness of the multi-coating PEDOT:PSS films I absence of acid treatment and after the treatment with 60 % HNO_3.

Number of PEDOT:PSS coatings	1	3	6	9
Thickness [nm], no acid	56	78	109	128
Thickness [nm], 60 % HNO_3	29	51	78	92

Table 3
Comparison of conductivity of a single PEDOT:PSS layer for acids, HNO_3, H_3PO_4, and H_2SO_4.

Conductivity Enhancement Technique	Conductivity [S/cm]
Nitric Acid (HNO_3) for 2 s, 100 % Concentration, 1 × PEDOT:PSS	1938
Phosphoric Acid (H_3PO_4) for 2 s, 100 % Concentration, 1 × PEDOT:PSS	278
Sulfuric Acid (H_2SO_4) for 2 s, 100 % Concentration, 1 × PEDOT:PSS	1515

As seen from Table 3, nitric and sulfuric acid outperform phosphoric acid by a factor of at least five, with nitric acid showing a slight advantage over phosphoric acid. The observed enhancements of conductivity hold consistent across different acid concentrations and treatment durations, even with the application of a 60 % acid concentration for 1 minute. Given that nitric acid consistently delivers the best results, our subsequent focus will center on the nitric acid process. When conducting experiments with nitric acid at a 100 % concentration (corresponding to the commercially available 14 M HNO_3), we explored different treatment durations: 1, 2, 3, 30, 40, and 60 seconds. Our findings revealed that varying the treatment time had only a minor effect on conductivity, with the 2-second treatment showing a slight advantage.

Our investigation then turns to the influence of nitric acid concentration on its ability to enhance conductivity. Given the well-known principle that more concentrated acid solutions tend to be more effective, we sought to ensure a fair comparison by extending the treatment time to 60 seconds for all acid concentrations. The outcomes of this study are presented in Table 4. Not surprisingly, the 1×PEDOT:PSS samples, showed that a 100 % (14 M) nitric acid concentration resulted in the highest conductivity of 2805 S/cm, while the lowest concentration of 20 % led to the lowest conductivity, of 193 S/cm. Interestingly, acid concentrations of 40 %, 60 %, and 80 % produced comparable results in terms of conductivity, between 2145 and 1823 S/cm.

In Fig. 4 and Table 5, we contrast the conductivity of PEDOT:PSS stacks subjected to 60 % nitric acid treatment with those without acid treatment, considering the number of layers.

Nitric acid treatment significantly reduces sheet resistance by approximately two orders of magnitude for all numbers of PEDOT:PSS coatings. Notably, the best result achieved is 15699 s/cm for 9×PEDOT:PSS layers treated with 60 % nitric acid. This result puts PEDOT:PSS on equal footing with conductivity of ITO reported recently of 13000 S/cm [37] and 16,600 S/cm [38]. It is important to highlight that this study builds upon our earlier research [1], pushing the analysis beyond the previous maximum of 6×PEDOT:PSS layers to now include 9 layers. The incorporation of these additional 3 layers leads to a threefold

Table 4
Conductivity as a function of HNO_3 acid concentration applied for 1 min.

Conductivity Enhancement Technique		Conductivity [S/cm]
1	× PEDOT:PSS + 100 % HNO_3 for 1 min	2564
1	× PEDOT:PSS + 80 % HNO_3 for 1 min	1772
1	× PEDOT:PSS + 60 % HNO_3 for 1 min	1578
1	× PEDOT:PSS + 40 % HNO_3 for 1 min	1276
1	× PEDOT:PSS + 20 % HNO_3 for 1 min	122

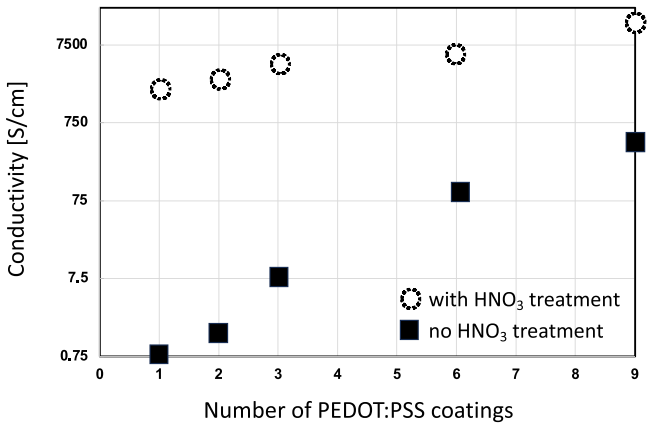

Fig. 4. The figure provides a comparison of conductivity on a logarithmic scale between the multilayer PEDOT:PSS stack treated with HNO_3 and the untreated stack.

Table 5
Conductivity of multilayer PEDOT:PSS layer stacks as a function of the number of layers with and without nitric acid treatment.

Conductivity Enhancement Technique	Conductivity w/ 60 % HNO_3 for 1 min [S/cm]	Conductivity w/o HNO_3 [S/cm]
1 × PEDOT:PSS	1842	0.8
3 × PEDOT:PSS	3771	7
6 × PEDOT:PSS	5753	101
9 × PEDOT:PSS	15,699	2072

enhancement in conductivity. Nevertheless, subsequent increases (more than 9 coatings) in the number of layers yield only marginal enhancements. The cross-sections of multi-layer PEDOT:PSS: without acid application and with acid application are depicted schematically in Fig. 5, indicating the final film thicknesses. It is evident that multi-layer PEDOT:PSS does not significantly increase the film thickness. For example, three layers of PEDOT:PSS (spun at 1500, 2000, and 3000 rpm) result in a thickness of 72 nm, which is only 7 nm more than a single layer spun at 2000 rpm, rather than the expected 150 nm (65 + 56 + 29 nm). Similarly, nine layers of PEDOT:PSS (spun at 1500, 2000, and seven times at 3000 rpm) yield a thickness of 119 nm, rather than the expected 324 nm (65 + 56 + 7 × 29 nm). It is also evident that acid treatment substantially reduces the overall film thickness in agreement with findings of ref. [10]

The extension from 6 to 9 layers, especially in the case of acid treatment, suggests that the extra 3 layers serve to compensate for the material loss incurred during the etch treatment. As described in more detail elsewhere [1], during the spin deposition of PEDOT:PSS, a vertical phase separation phenomenon occurs, segregating the PEDOT and PSS components. The resulting wet film accumulates conductive PEDOT strips at its base and a PSS-rich solution at the upper segment. The transition between PEDOT and PSS phases is, of course, not abrupt but gradual, with the highest concentration of PSS at the top and the lowest at the bottom, exhibiting an opposite behavior for PEDOT. With the application of each successive PEDOT:PSS layer, the PEDOT component of the subsequent coating permeates through the soluble PSS of the preceding layer, leading to the thickening and consolidation of the combined PEDOT phase at the base of the film. Following this, when acid treatment is applied, the upper portion of the layer containing the non-conductive PSS phase is eliminated. It is crucial to highlight that during the acid treatment process, a considerable portion of PSS inclusions within the PEDOT phase is removed, reducing the thickness of the film thereby improving the conductivity of the resultant layer, see Figs. 4 and 5.

Our attention now shifts to the potential of silver nanoparticles (Ag NP) to enhance the electrical conductivity of PEDOT:PSS. Given silver's inert nature, we introduced it using two methods: bulk doping, where Ag NP dispersion was mixed with PEDOT:PSS solution, and topical application after a soft bake of the PEDOT:PSS. Two sizes of Ag NP, ranging from 20 to 30 nm and 50–60 nm, were employed. Our experiments reveal that larger Ag nanoparticles consistently yield higher conductivity values. Table 6 compares bulk and topical applications of Ag NP for 1× PEDOT:PSS and 3×PEDOT:PSS.

Topical Ag NP application results in significantly higher conductivity compared to the bulk method, demonstrating a three-order-of-magnitude improvement. Hence, this method might be preferable in applications such as ReRAM cells where the presence of Cu or Ag at the surface is highly desirable [39–42].

This suggests that even in the case of noble metal nanoparticles, bulk

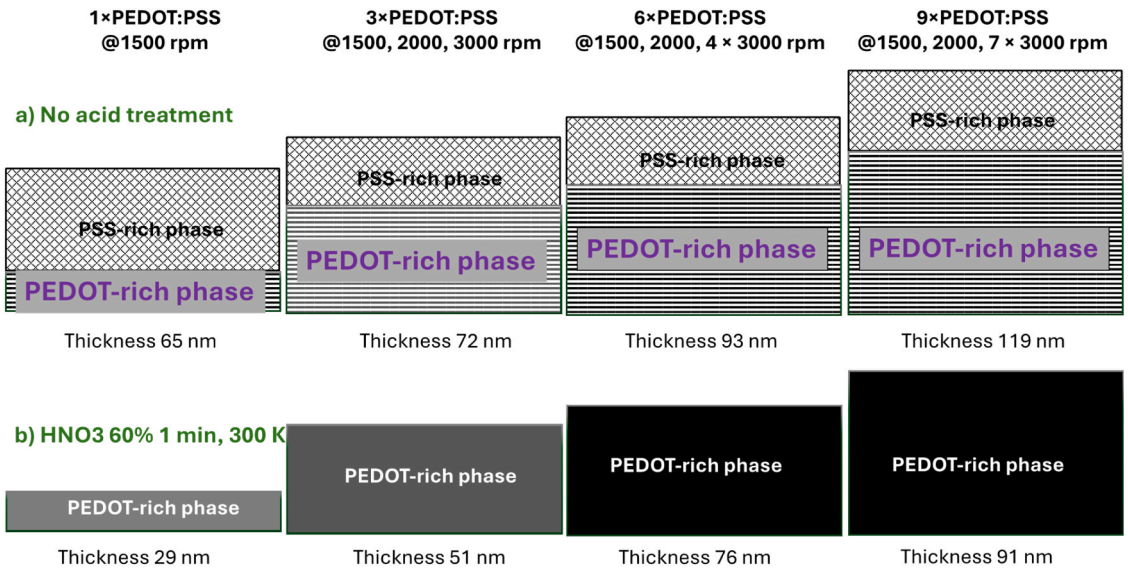

Fig. 5. Schematic depiction of cross-sections of multi-layer PEDOT:PSS: a) without acid application and b) with acid application (our baseline recipe of 60 % HNO_3 at room temperature). The thicknesses of the final films have been measured by AFM and Dektak profilometer and are indicated in the figure. Of course, there is no abrupt transition between the two phases, but rather a progressive one, with the highest concentration of PSS at the top and the lowest at the bottom, with the reverse behavior of the PEDOT.

Table 6
Conductivity of 1 × PEDOT:PSS and 3 × PEDOT:PSS with bulk and topical doping with Ag nanoparticles.

Conductivity Enhancement Technique	Conductivity [S/cm]
1 × PEDOT:PSS + 1 × 0.5 mg/ml Ag NP in Ethanol (Topical Application)	348
1 × [PEDOT:PSS + 0.5 mg/ml Ag NP]	0.3
3 × PEDOT:PSS + 3 × 0.5 mg/ml Ag NP in Ethanol (Topical Application)	1033
3 × [PEDOT:PSS + 0.5 mg/ml Ag NP]	4

doping with nanoparticles is ineffective due to potential issues such as inadequate accommodation of Ag NP within PEDOT:PSS and possible coating of Ag NP by PSS. To the best of our knowledge, there are no existing reports on the topical application of metal nanoparticles in PEDOT:PSS.

Given the inefficacy of bulk doping with Ag NP, we proceeded to compare the results with topical application of copper nanoparticles (Cu NP), a method utilized in our previous study. For 3×PEDOT:PSS layers, both Ag and Cu NP resulted in comparable conductivity values of 500–1073 S/cm and 507–750 S/cm, respectively. Additionally, both types of nanoparticles produced similar effects on conductivity for 3×PEDOT:PSS layers treated with 60 % HNO_3 acid. Therefore, it can be concluded that Cu nanoparticle doping offers an economically advantageous alternative to silver particle doping. As documented in the literature [12,13], both Ag and Au nanoparticles, when employed in bulk doping, result in comparable levels of conductivity enhancement in PEDOT:PSS films. Consequently, our earlier conclusion regarding the limited effectiveness of bulk doping compared to topical doping is likely applicable to gold nanoparticles, Au NPs, as well.

In Fig. 6, optical microscopy and AFM images showcase the 1×PEDOT:PSS 1500 rpm and 3×PEDOT:PSS 1500 rpm doped with Cu NPs. The Cu NPs (size ranging from 20 nm to 30 nm) are identifiable by their orange glint. According to the AFM measurements the root mean square surface roughness of 1×PEDOT:PSS was 2.01 nm and the surface roughness increased for multi-layer PEDOT:PSS to 2,42, 2,37, and 2.29 nm, for 3×PEDOT:PSS, 6×PEDOT:PSS, and 9×PEDOT:PSS, respectively.

Now, we delve into the finer details of nitric acid treatment. Various concentrations ranging from 0 % to 100 % and different treatment times were tested. The effectiveness of conductivity enhancement was found to be relatively independent of treatment time within the 1-second to 1-minute range. To ensure consistent treatment duration and minimize possible human errors, a baseline procedure of 1-minute duration was adopted, with similar results observed for 30-second and 40-second durations.

Additionally, the stability of nitric acid treatment over time was assessed. Samples were allowed to sit for several days, and conductivity was monitored periodically. The outcomes of the experiments are visually represented in Fig. 7. Over time, it becomes apparent that the conductivity experiences deterioration across all acid concentrations, eventually reaching a point of saturation and maintaining relatively constant values after approximately six days.

Fig. 8 regraphs the data from Fig. 7, representing sheet resistance degradation (D%) as defined by:

$$D\% = \frac{\text{conductivity} - \text{at} - \text{day measured} \; - \; \text{conductivity} - \text{just} - \text{after} - \text{being} - \text{manufactured}}{\text{conductivity} - \text{just} - \text{after} - \text{being} - \text{manufactured}} \tag{2}$$

It is notable from Fig. 8 that the sheet resistance exhibits its most stable performance at a 60 % concentration of nitric acid. Consequently, for the experiments discussed earlier, we adopted the 60 % nitric acid concentration as our baseline method.

The intriguing aspect of conductivity degradation over time following acid treatment prompted an investigation into its potential causes. One hypothesis proposed that the degradation might arise from a reaction between the PEDOT:PSS treated with acid and the ambient laboratory atmosphere. To validate this assumption, we created identical samples, placing some in the ambient laboratory atmosphere and others in a small vacuum chamber, from which the samples were removed for a brief period to measure sheet resistance and determine the conductivity.

Fig. 9 presents the results for samples stored in both ambient laboratory conditions and the vacuum chamber. Remarkably, there was no substantial difference observed in conductivity between the two environments. Consequently, we conclude that the degradation is not triggered by a reaction between the samples and the ambient atmosphere

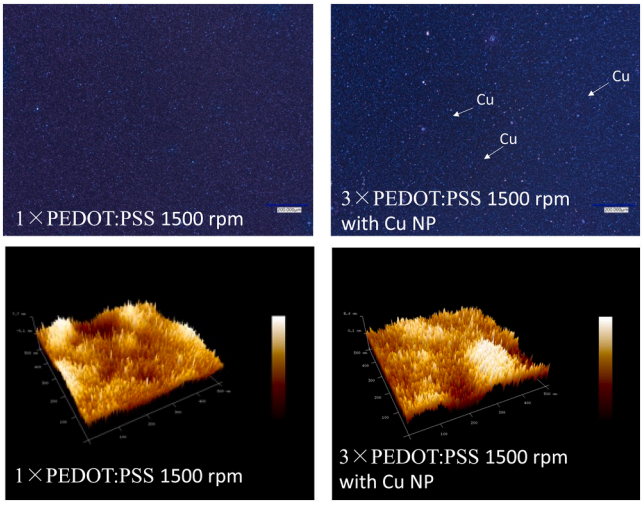

Fig. 6. Optical microscopy and AFM images showcase the 1×PEDOT:PSS 1500 rpm and 3×PEDOT:PSS 1500 rpm doped with Cu NPs. The Cu NPs (size ranging from 20 nm to 30 nm) are identifiable by their orange glint.

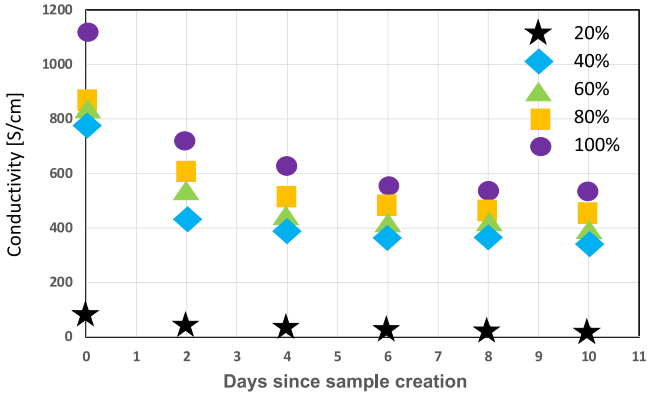

Fig. 7. Conductivity stability as a function of ambient exposure for 20 %, 40 %, 60 %, 80 %, 100 % nitric acid concentration.

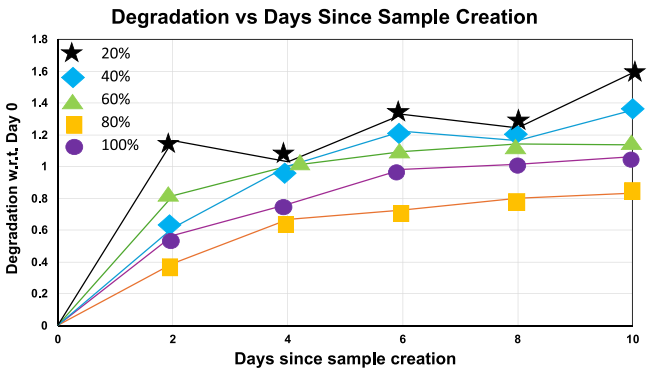

Fig. 8. Conductivity degradation as a function of ambient exposure for 20 %, 40 %, 60 %, 80 % nitric acid concentration.

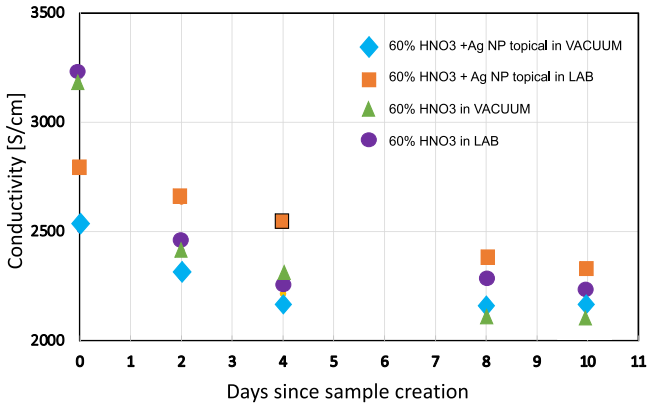

Fig. 9. Sheet resistance evolution as a function of time (days) for nitric acid treatment at concentration of 60 %,of HNO_3 with and without topical Ag NP doping in laboratory ambient and in vacuum chamber.

but rather stems from an internal reaction within the PEDOT:PSS material itself. This observation is fortuitous, considering the limited supply of nm-thin films for this reaction. It also elucidates why the degradation eventually reaches a saturation point over time.

The third approach aimed at enhancing the conductivity of PEDOT:PSS films involved introducing graphene on an oxidized Si wafer before PEDOT:PSS layer deposition. Two types of graphene were tested: a single large graphene monolayer and trilayer graphene, as described in the previous section. The sheet resistance for the graphene monolayer was measured at 20 kΩ/sq (which assuming a thickness of 1 nm would correspond to a conductivity of 500 S/cm), while the trilayer graphene exhibited significantly lower resistance at 50 Ω/sq (which assuming of thickness of the trilayer of 4 nm would correspond to a conductivity of 50,000 S/cm).

It should be noted that when using trilayer graphene, adhesion issues with PEDOT:PSS were encountered. We addressed this challenge by subjecting the trilayer graphene to plasma treatment, significantly improving PEDOT:PSS adhesion to the trilayer graphene. This adhesion improvement came, however, at a cost, as the conductivity of the trilayer graphene deteriorated considerably. Moreover, conductivity values for PEDOT:PSS with the graphene trilayer displayed a highly non-uniform distribution of conductivity, ranging from 9276 S/cm to 130 S/cm depending on the location of the measurement. Notably, achieving conductivity values as high as 9276 S/cm at the higher end of the range through plasma treatment of trilayer graphene presents promising avenues for future exploration.

It's worth noting that the higher end of the conductivity spectrum for plasma-treated trilayer graphene, with values as high as 9276 S/cm, offers some optimism for potential future studies. Effectively addressing the non-uniformity issue remains feasible, particularly considering that handling trilayer graphene is more manageable than transferring a graphene monolayer onto a substrate. However, it is important to recognize that trilayer graphene requires a film provided on oxidized Si substrates by the supplier (Graphenea [33]), which imposes constraints on autonomy in the manufacturing process, particularly on commercially avialable wafer sizes. Nevertheless, we produced a single sample of 6×PEDOT:PSS on plasma-treated trilayer graphene, resulting in a conductivity of 6,800 S/cm. One favorable outcome of this result is the absence of sheet resistance nonuniformity across the wafer. On the other hand, a graphene monolayer combined with 9 layers of PEDOT:PSS yielded a respectable conductivity 2,130 S/cm. However, it still falls short of the the conductivity achieved by 9×PEDOT:PSS treated with 60 % nitric acid, which resulted in σ=15,699 S/cm.

Similar to metal nanoparticles, adding graphene—in monolayer and triple-layer versions—brings advantages of its own, but it doesn't work in concert with nitric acid treatment, just like silver nanoparticles do. The optimization of the nitric acid treatment addresses the deterioration in conductivity brought on by both ambient-induced and ambient-independent effects, as well as film aging. A significant finding in this study is the efficacy of the straightforward approach: combining multiple PEDOT:PSS depositions with optimized nitric acid treatment, while considering the impact of acid concentration and acid treatment time. This approach surpasses the efficacy of complex methods involving metal nanoparticles and graphene layers while providing a simpler and cost-effective means of enhancing PEDOT:PSS conductivity. Compared to a single-layer PEDOT:PSS of the same thickness, the optimized multilayer PEDOT:PSS treated with optimized nitric acid shows a enhancement of conductivity from 0.18 S/cm to 16,427 S/cm, marking a tenfold improvement over the highest conductivity of 1575 S/cm (measured sheet resistance of 62Ω/sq) achieved with 6 PEDOT:PSS layers and topical dispersion of Cu nanoparticle doping reported in our previous work [1].

Finally, let's explore the combined effects of multiple enhancement methods. To our knowledge, the combined effects of different enhancement methods have been not yet reported Firstly, we examine the combination of nitric acid treatment and silver nanoparticle doping. For 3×PEDOT:PSS, HNO_3 treatment alone results in a conductivity of 3846 S/cm, while the addition of Ag NP as a topical application yields similar results. An outlier at 7692 S/cm has been noted, attributed to the use of a newly shipped PEDOT:PSS (refer to the remark at the end of this section).

Hence, it can be concluded that the addition of metal nanoparticles does not yield a significant improvement over nitric acid treatment alone.

An intriguing combination of enhancement methods involves the simultaneous application of nitric acid treatment and graphene insertion. While each method independently significantly enhances the conductivity, their combined effect seems negligible. For instance, a 9×PEDOT:PSS layer treated with nitric acid achieves a conductivity of 15,699 S/cm, and with the addition of a graphene monolayer, the conductivity only slightly increases to 15,926 S/cm. Overall, nitric acid treatment alone proves to be the most effective approach for enhancing PEDOT:PSS conductivity, with combinations offering no additional benefits. Furthermore, the nitric acid method is the least expensive and least complex when compared to metal nanoparticle doping and graphene insertion.

As a note on the margin, we would like to discuss an observation mentioned earlier in the text. A recent shipment of PEDOT:PSS from Sigma-Aldrich consistently displayed a higher conductivity, approximately 2–3 times higher than the initial batch received approximately a year ago. While the new material does show a slight improvement in conductivity, the observed trends and dependencies remain consistent with those of the older material. Sigma-Aldrich [43] has not shared any details regarding the process changes that led to this conductivity improvement.

4. Conclusions

A record high conductivity of more than 15,000 S/cm for PEDOT:PSS has been reported, putting it on par with the conductivity of ITO films [37,38]. The simplest, cost-effective, and process-stable method involves creating a nine-layer PEDOT:PSS structure treated with HNO_3 at 300 K, yielding a conductivity of 15,699 S/cm. Combining this method with additional enhancements, such as graphene or metal nanoparticles, brings only marginal improvements, if any, and does not justify the added complexity and cost. For example, adding a graphene monolayer to the nine-layer PEDOT:PSS stack and treating it with HNO_3 boosts the conductivity to 15,926 S/cm, which is only a slight improvement. However, it's worth noting that the electrical conductivity of acid-treated PEDOT:PSS layers degrades over time, albeit at a modest rate, stabilizing after a few days. A trilayer graphene combined with a single PEDOT:PSS layer shows a respectable conductivity of up to 9,276 S/cm but suffers from adhesion issues, which can be addressed by surface plasma treatment. This treatment, however, results in non-uniform conductivity, producing a wide scatter between 130 and 9,276 S/cm.

In the realm of metal nanoparticle doping, we have observed that topical doping by NPs outperforms bulk doping. Notably, Cu nanoparticles, which are unsuitable for bulk doping, are as effective as noble metal nanoparticles when used topically, offering a more cost-effective alternative. Regarding graphene's role in enhancing conductivity, we found that trilayer graphene, despite being more affordable than monolayer graphene, faces adhesion challenges with the PEDOT:PSS layer. While adhesion issues can be mitigated through topical plasma treatment, this intervention compromises the uniformity of sheet resistance and degrades electrical conductivity gains. Nevertheless, the trilayer graphene method shows promise for enhancing conductivity, pending further research and development.

We expect that the knowledge acquired through our investigation of various methods to enhance conductivity, as outlined in this paper, will aid other researchers in identifying the most appropriate strategies to improve the conductivity of organic polymers in their specific areas of study.

Disclaimer

In this work no plasma sample from human have been used.

Author statement

We, the authors, declare that all the listed authors have made significant contributions to the research and preparation of this manuscript. Specifically, M.O. was responsible for the study design and supervision, [A.C.and A.D.] conducted the experiments and collected the data, and [M.O. performed the data analysis and drafted the manuscript. The remaining authors contributed to some manufacturing in the clean room and electrical characterization of the polymer films. All authors have reviewed and approved the final version of the manuscript.

CRediT authorship contribution statement

Amrita Chakraborty: Writing – original draft, Supervision, Investigation. **Marius K Orlowski:** Writing – review & editing, Supervision, Methodology, Conceptualization. **Anshu Madwesh:** Investigation. **Calvin Hong:** Investigation. **Sheena Deivasigamani:** Investigation. **Aaron DiFilippo:** Visualization, Validation, Investigation.

Declaration of Competing Interest

We, the authors, declare that we have no commercial interests associated with this work. Our endeavors are solely driven by scientific exploration and the pursuit of knowledge.

Data Availability

No data was used for the research described in the article.

Acknowledgements

We express our gratitude to Prof. Scot Ransbottom, Prof. Kenneth Schulz, and Dr. Don Leber for their invaluable assistance in facilitating this work and providing guidance in navigating clean room issues.

References

[1] A. Chakraborty, D. Herrera, Payton Fallen Hall, N. Bampton, T. Olivero, M. Orlowski, Conductive organic electrodes for flexible electronic devices, Sci. Rep. 13 (2023) 4125.
[2] V. Ratautaite, A. Ramanavičienė, Y. Oztekin, J. Voronovic, Z. Balevicius, L. Mikoliunaite, A. Ramanavicius, Electrochemical stability and repulsion of polypyrrole film, Colloids Surf. A: Physicochem. Eng. Asp. 418 (2013) 16–21.
[3] J. Ouyang, Q. Xua, C.-W. Chua, Y. Yanga, G. Lib, J. Shinar, On the mechanism of conductivity enhancement in poly(3,4-ethylenedioxythiophene):poly(styrene sulfonate) film through solvent treatment, Polymer 45 (2004) 8443–8450.
[4] Y. Xie, J. Ouyang, PEDOT:PSS films with significantly enhanced conductivities induced by preferential solvation with cosolvents and their application in polymer photovoltaic cells, J. Mater. Chem. 21 (2011) 4927.
[5] Y. Xia, K. Sun, J. Ouyang, Highly conductive poly(3,4-ethylenedioxythiophene): poly(styrene sulfonate) films treated with an amphiphilic fluoro compound as the transparent electrode of polymer solar cells, Energy Environ. Sci. 5 (2012) 5325.
[6] K. Sun, S. Zhang, P. Li, Y. Xia, X. Zhang, D. Du, F.H. Isikgor, J. Ouyang, Review on application of PEDOTs and PEDOT:PSS in energy conversion and storage devices, J. Mater. Sci: Mater. Electron (2015), https://doi.org/10.1007/s10854-015-2895-5.
[7] Z. Fan, P. Li, D. Du, J. Ouyang, Significantly enhanced thermoelectric properties of PEDOT:PSS films through sequential post-treatments with common acids and bases, Adv. Energy Mater. 7 (2017) 1602116, https://doi.org/10.1002/aenm.201602116.
[8] X. Fan, N.E. Stott, L. Chue, W. Song, J. Zeng, Y. Li, J. Ouyang, PEDOT:PSS materials for optoelectronics, thermoelectrics, and flexible and stretchable electronics, J. Mater. Chem. A 11 (2023) 18561.
[9] N. Kim, S. Kee, S.H. Lee, B.H. Lee, Y.H. Kahng, Y.-R. Jo, B.-J. Kim, K. Lee, Highly Conductive PEDOT:PSS Nanofibrils Induced by Solution-Processed Crystallization, Adv. Mater. 26 (2014) 2268–2272.
[10] Ch Yeon, S.J. Yun, J. Kim, J.W. Lim, PEDOT:PSS films with greatly enhanced conductivity via nitric acid treatment at room temperature and their application as Pt/TCO-free counter electrodes in dye-sensitized solar cells, Adv. Electron. Mater. 1 (2015) 150012.
[11] Z. Xiong, C. Dong, H. Cai, C. Liu, X. Zhang, Composite inks of poly(3,4-ethylenedioxytiophene)/poly(styrenwsulfonate)/silver nanoparticles and electric/optical properties of ink-jet-printed thin films, Mater. Chem. Phys. 141 (2013) 416–422.
[12] D.S. Patil, S.A. Pawar, J. Hwang, J.H. Kim, P.S. Patil, J.C. Shin, Silver incorporated PEDOT: PSS for enhanced electrochemical performance, J. Ind. Eng. Chem. 42 (2016) 113–120.
[13] R.-C. Zhang, D. Sun, R. Zhang, W.-F. Lin, M. Macias-Montero, J. Patel, S. Askari, C. McDonald, D. Mariotti, P. Maguire, Gold nanoparticle-polymer nanocomposites synthesized by room temperature plasma and their potential for fuel cell electrocatalytic application, Sci. Rep. 7 (2017) 46682.
[14] O.A. Ghazy, M.M. Ibrahim, F.I. Abou-Elfadl, H.M. Hosni, E.M. Shehata, N. M. Dehiedy, M.R. Balboul, PEDOT:PSS incorporated silver nanoparticles prepared by gamma radiation for the application in organic solar cells, J. Rad. Res. Appl. Sci. 8 (2015) 166–172.
[15] L.Q. Pham, J.H. Sohn, C.W. Kim, J.H. Park, H.S. Kang, B.C. Lee, Y.S. Kang, Copper nanoparticles incorporated with conducting polymer: effects of copper concentration and surfactants on the stability and conductivity, J. Colloid Interface Sci. 365 (2012) 103–109.
[16] W. Wang, F. Qin, X. Jiang, X. Zhu, L. Hu, C. Xie, L. Sun, W. Zeng, Y. Zhou, Patterning of PEDOT:PSS via nanosecong ablation and acid treatment for organic solar cells, Org. Electron. 87 (2020) 105954.
[17] Z. Hu, J. Wang, Z. Wang, W. Gao, Q. An, M. Zhang, X. Ma, J. Wang, J. Miao, C. Yang, F. Zhang, Semitransparent ternary nonfullerene polymer solar cells exhibiting 9.40% efficiency and 24.6% average visible transmittance, Nano Energy 55 (2019) 424–432.
[18] Z. Hu, Z. Wang, Q. An, F. Zhang, Semitransparent polymer solar cells with 12.37% efficiency and 18.6% average visible transmittance, Sci. Bull. 65 (2) (2020) 131–137.
[19] X. Zhang, J. Wu, J. Wang, J. Zhang, Q. Yang, Y. Fu, Z. Xie, Highly conductive PEDOT:PSS transparent electrode prepared by a post-spin-rinsing method for efficient ITO-free polymer solar cells, Sol. Energ. Mat. Sol. Cells 144 (2016) 143–149.

[20] D. Yoo, J. Kim, J.H. Kim, Direct synthesis of highly conductive PEDOT:PSS/graphene composites and their applications in energy harvesting systems, Nano Res. 7 (5) (2014) 717–730.
[21] M. Zhang, W. Yuan, B. Yao, C. Li, G. Shi, Solution-processed PEDOT:PSS/graphene composites as the electrocatalyst for oxygen reduction reaction, ACS Appl. Mat. Inter. 6 (2014) 3587–3593.
[22] P.C. Mahakul, K. Sa, B. Das, B.V. Subramaniam, S. Saha, B. Moharana, J. Raiguru, S. Dash, J. Mukherjee, P. Mahanadia, Preparation and characterization of PEDOT:PSS/reduced graphene oxide-carbon nanotubes hybrid composites for transparent electrode applications, J. Mater. Sci. 52 (2017) 5696–5707.
[23] D.P. Kepic, Z.M. Markovic, S.P. Jovanovic, D.B. Peruško, M.D. Budimir, I. D. Holclajtner-Antunovic, V.B. Pavlovic, B.M. Todorovic-Markovic, Preparation of PEDOT:PSS thin films doped with graphene and graphene quantum dots, Synth. Met. 198 (2014) 150–154.
[24] D. Liu, M.M. Rahman, C. Ge, J. Kima, J.-J. Lee, Highly stable and conductive PEDOT:PSS/graphene nanocomposites for biosensor applications in aqueous medium, N. J. Chem. 41 (2017) 15458–15465.
[25.] S.H. Ko, S.W. Kim, Y.J. Lee, Flexible sensor with electrophoretic polymerized graphene oxide/PEDOT:PSS composite for voltametric determination of dopamine concentration, Sci. Rep. 11 (2021) 21101.
[26] F.P. Du, N.-N. Cao, Y.-F. Zhang, P. Fu, Y.-G. Wu, Z.-D. Lin, R. Shi, A. Amini, C. Cheng, PEDOT:PSS/graphene quantum dots with enhanced thermoelectric properties via strong interfacial interactions and phase separation, Sci. Rep. 8 (2018) 6441.
[27] M.A.S. Badri, N.F. Noor, A.R. Zain, M. MatSalleh, T.H. Tengku Aziz, Exfoliated graphene-alkaline lignin-PEDOT:PSS composite as a transparent conductive electrode, Nanomat. Nanotechnol. 11 (2021) 1–8.
[28] S.K. Nemani, D. Chen, M.H. Mohamed, H. Sojoudi, Stretchable and Hydrophobic Electrochromic Devices Using Wrinkled Graphene and PEDOT:PSS', J. Nanomat (2018) 3230293.
[29] G.J. Adekoya, R.El Sadiku, S.S. Ray, Nanocomposites of PEDOT:PSS with graphene and its derivatives for flexible electronic applications: a review, Macromol. Mater. Eng. 306 (2021) 2000716.
[30] O. Faruk, B. Adak, Recent advances in PEDOT:PSS integrated graphene and MXene-based composites for electrochemical supercapacitor applications, Synth. Met. 297 (2023) 117384.
[31] A. Popov, B. Brasiunasa, L. Mikoliunaite, G. Bagdziunasa, A. Ramanaviciusa, A. Ramanaviciene, Comparative study of polyaniline (PANI), poly(3,4-ethylenedioxythiophene) (PEDOT) and PANI-PEDOT films electrochemically deposited on transparent indium thin oxide based electrodes, Polymer 172 (2019) 133–141.
[32] A. Popov, B. Brasiunas, A. Damaskaite, I. Plikusiene, A. Ramanavicius, A. Ramanavičienė, Electrodeposited gold nanostructures for the enhancement of electrochromic properties of PANI–PEDOT film deposited on transparent electrode, Polymers 12 (2020) 2778, https://doi.org/10.3390/polym12122778.
[33] ⟨https://www.graphenea.com/products/graphene-on-your-substrate⟩.
[34] J. Olivier, B. Sevet, M. Vergnolle, M. Mosca, G. Gary, Stability/instability of conductivity and work function changes of ITO thin films, UV-irradiated in air or vacuum: Measurements by the four-probe method and by Kelvin force microscopy, Synth. Met. 122 (1) (2001) 87–89.
[35] J.K. Kim, S.J. Yun, J.M. Lee, J.W. Lim, Effect of rf-power density on the resistivity of Ga-doped ZnO film deposited by rf-magnetron sputter deposition technique, Curr. Appl. Phys. 10 (2010) 451.
[36] J.K. Kim, J.M. Lee, J.W. Lim, J.H. Kim, S.J. Yun, Semi-transparent amorphous silicon solar cells using a thin p-Si layer and a buffer layer, Jpn. J. Appl. Phys. 49 (2010) 04DP09.
[37] C.G. Granqvist, Sol. Energy Mater. Sol. Cells 91 (2007) 1529.
[38] Y.F. Li, X. Fan, C. Shen, X. Shi, P.C. Li, K. Hui, J.P. Fan, K. Kang, T. Zhang, L. Qian, Adv. Funct. Mater. 32 (2022) 2203641.
[39] T. Liu, Y. Kang, M. Verma, M. Orlowski, IEEE Electron Dev. Lett. 33 (2012) 429.
[40] Y. Kang, H. Ruan, R.O. Claus, J. Heremans, M. Orlowski, Nanoscale Res. Lett. 11 (2016) 179.
[41] M.S. Al-Mamun, A. Chakraborty, M. Orlowski, Analysis of the 4lectrical ReRAM device degradation induced by thermal cross-talk, Adv. Electron. Mater. 9 (4) (2023) 2201081.
[42] A. Chakraborty, M.S. Al-Mamun, M.K. Orlowski, Thermal Reliability Issues in ReRAM Memory Arrays chapter in the book entitled: Memristors - the Fourth Fundamental Circuit Element - Theory, Device, and Applications, edited by Dr. Yao-Feng Chang, IntechOpen, September 2023, DOI: 10.5772/intechopen.1001963.
[43] Sigma Aldrich, ⟨https://www.sigmaaldrich.com/US/en/product/aldrich/774103⟩.